

Theory of adiabatic Hexaamminecobalt-Self-Exchange

R. G. Endres, M. X. LaBute, D. L. Cox

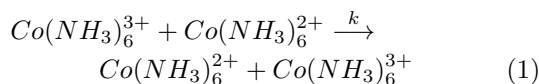
Department of Physics, University of California, Davis, CA 95616

(Dated: March 3, 2019)

We have reexamined the thermally induced $Co(NH_3)_6^{2+/3+}$ [Co(II/III)] redox reaction using the first principles density-functional-theory method, semiclassical Marcus theory, and known charge transfer parameters. We confirm a previously suggested mechanism involving excited state (2E_g) of Co(II) which becomes lower than the ground state (${}^4T_{1g}$) in the transition state region. This lowers the transition state barrier considerably by $\sim 6.9kcal/mol$ and leads to a spin-allowed and adiabatic electron exchange process. Our calculations are consistent with previous experimental results regarding the spin-excitation energy (${}^3T_{1g}$) of Co(III), and the fact that an optical absorption peak (2E_g) of the Co(II) species could not be found experimentally. Our rate is of order $6 \cdot 10^{-3}(Ms)^{-1}$ and hence 2 orders of magnitude faster than determined previously by experiments.

I. INTRODUCTION

The experimental rate determination and theoretical understanding of the $Co(NH_3)_6^{2+/3+}$ redox reaction in aqueous solution



has been a great intellectual challenge for several decades. Despite substantial effort, the mechanism of the rate is still an unsolved problem. Is the reaction spin-forbidden and diabatic or are spin-excited states thermally accessible which would possibly lead to a spin-allowed, adiabatic reaction?

Experimental studies in the early 1960s suggested an extremely slow rate of $k = 1.6 \cdot 10^{-10}(Ms)^{-1}$ [1] at 64.5 C and 1 M ionic strength using radiocobalt ${}^{60}C$ as a tracer. Unfortunately, side reactions involving hydrolysis of the complexes, which contribute to the rate, have not correctly been taken into account. In the 1980s a detailed analysis of previous data using the Marcus correlation[2] led to a much higher estimate of $1 \cdot 10^{-5}(Ms)^{-1}$ [3], and subsequent experiments labeling the ammonia ligands with ${}^{15}N$ (which can be assayed by NMR of the ammine protons and make it possible to trace side reactions) gave about $6 \cdot 10^{-6}(Ms)^{-1}$ at 40 C and 2.5 M ionic strength [4]. An estimate of the rate at normal conditions (25 C and 1M ionic strength) gives $\lesssim 5 \cdot 10^{-7}(Ms)^{-1}$ [5, 6, 7, 8]. These results can be expected to be rather trustworthy, because they are, as expected, similar to the rate of a closely related and well understood system, $Coen_3^{3+/2+}$, which has a rate of $5.2 - 7.7 \cdot 10^{-5}(Ms)^{-1}$ [9]. Furthermore, an early but less influential measurement of $Co(NH_3)_6^{2+/3+}$ in liquid NH_3 (and hence not suffering from hydrolytic side reactions) indicated a similar rate of order $10^{-5}(Ms)^{-1}$ [10].

Briefly, previous results of theory mainly by Buhks *et al* (1978) [11] and Newton (1986,1991) [8, 12] indicate that the reaction involves the ground state species low-spin $Co(NH_3)_6^{3+}$, ${}^1A_{1g}$ [Co(III,S=0)], and high-spin $Co(NH_3)_6^{2+}$, ${}^4T_{1g}$ [Co(II,S=3/2)]. The transition

states, ${}^3T_{1g}$ [Co(III,S=1)] and 2E_g [Co(II,S=1/2)], were to high in energy to be thermally populated. This led to a spin-forbidden (only possible by weak spin-orbit coupling), diabatic reaction with a rate constant of about 4 orders of magnitude too small compared to experiment. However, work by Larsson *et al* (1985) stressed that the ground state-excited state energy separations at the transition state have to be considered, not at the equilibrium geometries. Including Jahn-Teller (JT) stabilization energies for the excited states, this led in particular to a substantial energetic lowering of Co(II,S=1/2) relative to Co(II,S=3/2). Although this made the reaction spin-allowed, their work suffered from inconsistent data from different electronic structure codes. Furthermore, the rate constant was not determined.

In this paper we show that the thermal activation barrier for the spin-allowed reaction between Co(III,S=0) and Co(II,S=1/2) [total spin S in units of \hbar] is drastically lowered ($\sim 6.9kcal/mol$) compared to the spin-forbidden reaction between Co(III,S=0) and Co(II,S=3/2). Unlike previously believed, the JT-distorted spin-excited Co(II,S=1/2) and the ground state Co(II,S=3/2) are near degenerate. Hence the reaction is spin-allowed and adiabatic. Our results are based on the density functional theory (DFT)[13] code SIESTA[14] which we use to calculate spin-excited states of isocharge molecular species and potential energy surfaces (PESs). Since DFT is a ground state theory, excitation energies obtained from ground state energy differences of species with different total spin are expected to be rather good. The DFT method has the advantage over Hartree-Fock methods that certain correlations are already build in. From the PESs we determine the activation barrier and provide a new estimate of the rate constant utilizing previously estimated quantities like the e_g - electronic coupling $H_{DA} = {}_D \langle e_g | H | e_g \rangle_A$ between donor D and acceptor A molecular species, the outer-sphere contribution to the reaction barrier E_{out}^\ddagger , and the preequilibrium constant K_{equ} . Although our excitation energy of Co(III), $\Delta E^{3+|_{equ}} = 13,120cm^{-1}$, is in rather good agreement with the experimental value, we deemphasize the absolute numerical values of excitation energies. In-

lations exploiting that DFT usually stabilizes high-spin over low-spin states. If Co(II) has a low-spin ground state, this would also explain why the optical absorption ${}^2E_g \leftarrow {}^4T_{1g}$ has not been observed.

The paper is organized as follows. In section II we review further experimental and previous theoretical efforts in more detail. In section III we introduce the DFT code SIESTA and explain our computational methods (section III A), as well as present the calculation of the PESs (section III B). In section IV we provide a new estimate of the spin-allowed hexaammine self-exchange reaction based on our insights from the PESs and discuss our results. Finally, we summarize in section V.

II. REVIEW OF PREVIOUS EFFORTS

In this section further experimental facts about the single complexes and a more detailed review of past theoretical efforts are presented.

It is well accepted that $Co(NH_3)_6^{3+}$ [Co(III)] is a stable low-spin (S=0) compound, while it is *assumed* that $Co(NH_3)_6^{2+}$ [Co(II)] is high-spin (S=3/2). There are several reasons for this. First it is known from ${}^{59}Co$ NMR studies that the related system, $Co(H_2O)_6^{3+}$, shows no sign of exchange with paramagnetic species[15] and hence is low-spin. This is also expected to be true for Co(III), since it has an even larger ligand-field favoring low-spin. X-ray diffraction data of related crystals shows further a drastic difference of the Co-N bond distances ($\approx 0.22\text{\AA}$ [5, 16]) between Co(II) and Co(III). From this it was concluded that the ligand-field of Co(II) must be much smaller resulting in high-spin. Additionally, the optical excitation spectrum of Co(III) could be fully characterized including $d-d$ spin-forbidden transitions. This is different than Co(II), where it could not be measured successfully. It is further experimentally supported that the $Co(NH_3)_6^{2+/3+}$ self-exchange reaction occurs as outer-sphere. This is due to a rather slow ligand exchange rate of Co(III). There is considerable thermodynamic and kinetic stability, which arises from effective σ -donation into empty e_g -shells[17].

The theoretical effort is conveniently discussed in the context of the separable semi-classical transition-state model[18]

$$k_{et} = K_{equ}\nu_{eff}\kappa_{el}\Gamma_n\exp(-\beta G^\ddagger). \quad (2)$$

In this equation, K_{equ} is the preequilibrium factor describing the probability to form a precursor compound, ν_{eff} is an effective nuclear attempt frequency to reach the transition state (TS), $\kappa_{eq} \leq 1$ is the electronic transmission coefficient evaluated at the TS and averaged over all possible precursor compounds, $\Gamma_n \geq 1$ is the nuclear tunneling factor, and the Boltzmann factor (classical Franck-Condon factor) gives the probability to reach the TS with activation free-energy G^\ddagger ($\beta = 1/(k_B T)$). For the further

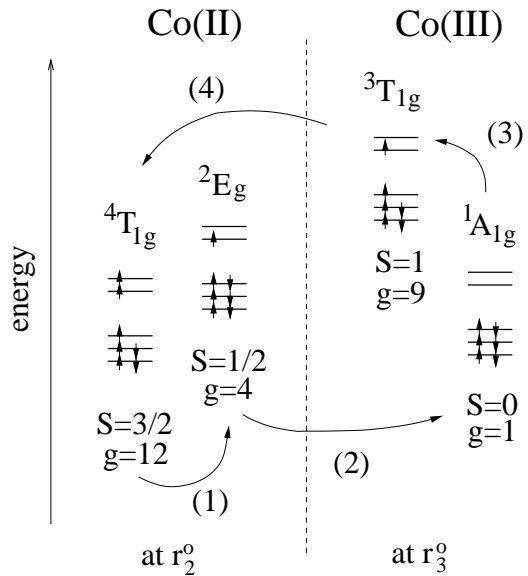


FIG. 1: Introduction of the ground state ${}^4T_{1g}$ [${}^1A_{1g}$] and first excited state 2E_g [${}^3T_{1g}$] of Co(II) [Co(III)], their irreducible representations, total spin S [\hbar], degeneracy g, and possible couplings (1) to (4). The energy ordering corresponds to the equilibrium Co-N bond lengths r_2^0 and r_3^0 of Co(II,S=3/2) and Co(III,S=0), respectively.

states in figure 1, i.e. their group theoretical representations, total spin S, degeneracy g, and possible couplings (1) to (4). The couplings (1) and (3) are due to spin-orbit coupling or thermal population at finite temperature T, (2) and (4) are mainly due to mixing of the electronic e_g -orbitals of Co(II) and Co(III) mediated by their ligands when a precursor state is formed.

It has been known for about 50 years that extraordinarily slow rates can often be attributed to small Franck-Condon nuclear overlaps. These originate from large changes in the metal-ligand bond length in the first coordination sphere[19]. This seemed to apply also to the case at hand, if one assumes an adiabatic reaction ($\kappa_{el} \approx 1$) "neglecting" the spin-forbiddenness. However, a first detailed theoretical study by E. Buhks and co-workers using perturbation theory in the weak spin-orbit coupling to admix spin-excited states shows that the electronic factor is very diabatic, $\kappa_{el} \approx 10^{-4}$ [11]. This makes the rate constant too small.

Orgel[20] and by Stynes and Ibers[21] put out an idea that the reaction could involve thermally excited Co(II,S=1/2) making it spin-allowed. Larsson *et al* [22] went further and argued that the excited states can become much lower in energy near TS. The important quantities are the energy difference between first excited state and ground state of Co(II) and Co(III) as a function of the Co-N bond length r

$$\Delta E^{3+}(r) = E({}^3T_{1g}) - E({}^1A_{1g}) \quad (3)$$

$$\Delta E^{2+}(r) = E({}^2E_g) - E({}^4T_{1g}) \quad (4)$$

In the case of Co(III) the lowering enhances somewhat the admixture to the ground state, while in case of Co(II), 2E_g becomes even lower than ${}^1A_{1g}$ circumventing the spin-barrier. Their argument is based on Born-Oppenheimer potential energy surfaces (PES) calculated both with *ab initio* Hartree-Fock (HF) and semi-empirical INDO-CI methods including e_g JT effects for both excited states. Unfortunately their result was not convincing, since the HF calculation predicts the wrong ground state for Co(III), while the INDO-CI excitation energy $\Delta E^{2+}|_{equ} = 2,000 - 3,000 \text{ cm}^{-1}$ was much lower than the generally believed $9,000 \text{ cm}^{-1}$ [11], although there is no experimental evidence for this value. There has been no absorption found in this region. On the other hand, the excitation energy of Co(III) is known from experiment to be $13,700 \text{ cm}^{-1}$ [23] at the Co(III) equilibrium configuration. Since their calculated value $\Delta E^{3+}|_{equ} = 14,800 \text{ cm}^{-1}$ is too large by an amount $c \approx 1,100 \text{ cm}^{-1}$, the PES from INDO-CI were corrected according to

$$\Delta E^{3+} \rightarrow \Delta E^{3+} - c \quad (5)$$

$$\Delta E^{2+} \rightarrow \Delta E^{2+} + c. \quad (6)$$

It was noted that the semi-empirical INDO-CI method is generally very successful in calculating spectra of transition-metal complexes at fixed geometries, but not so in predicting molecular geometries[24].

In 1991, Newton carried out new *ab initio* calculations at both the SCF(UHF) and correlated (UMP2) level. Using an empirical correction factor as large as $c = -6,000 \text{ cm}^{-1}$ (HF generally favors high-spin), he estimated the excitation energies at the transition state to be $\Delta E^{3+} = 8,800 \text{ cm}^{-1}$ and $\Delta E^{2+} = 5,300 \text{ cm}^{-1}$, and concluded that thermally excited pathways are not competitive to the spin-forbidden ground state pathway at room temperature (RT). This left the problem unsolved.

III. AB INITIO CALCULATIONS

A. Method

Our results of the inner-sphere activation barrier are based on PESs obtained from the fully *ab initio* code SIESTA[14] based on density functional theory (DFT). SIESTA uses Troullier-Martins norm-conserving pseudo potentials[25] in the Kleinman-Bylander form[26]. For cobalt, we included spin-polarization and non-linear core corrections[27] to account for a spin-dependent exchange splitting and correlation effects between core and valence electrons, respectively. Relativistic effects are included for the core electrons in the usual scalar-relativistic approximation (mass-velocity and Darwin terms) and by averaging over spin-orbit coupling terms, while no spin-orbit coupling is included for the 4s and 3d valence electrons. This has the computational advantage that spin

of the total energy are less crucial when one is interested in total energy differences. SIESTA uses a local basis set of pseudo atomic orbitals (PAO) of multiple ζ -type. The first- ζ orbitals are produced by the method by Sankey and Niklewski[28], while the higher- ζ orbitals are obtained from the split valence method well known from quantum chemistry. Polarization orbitals can also be included. We used a double- ζ basis set with polarization orbitals (DZP), as well as the generalized gradient approximation (GGA) in the version by Perdew, Burke and Ernzerhof[29] for the exchange-correlation energy functional. The charge densities are calculated on a real space grid, where the fineness of the grid corresponds to an energy cut-off 80 Ry.

Before going into the details of how we obtained the PESs plots, we outline the main ingredients of our calculations.

- Our calculations rest on the fixed-spin method within the spin-polarized DFT frame work. Two different Fermi energies, one for spin-up and one for spin-down, are adjusted in a self-consistent way in order to obtain the ground state of a desired total spin. If a ground state of a certain spin is higher than the ground state of a different spin, then we know the former as the excited state and the latter one as the true ground state. Nevertheless, there might be several states within a spin-manifold which differ in orbital symmetry. Since the DFT method is based on the variational principle, we obtain the state of a system with a certain total spin which has the lowest energy[30]. Our excitation energies are extracted from total energy differences using the well-established self-consistent-field method (Δ SCF)[31]. This gives generally reliable results for molecules since final state effects are included.
- The amines are treated as rigid bodies, i.e. the N-H bond lengths and the H-N-H bond angles stay the same throughout all our calculations. This is justified, since the vibrational frequencies of covalent bonds (N-H) are about one order of magnitude higher than the metal-ligand stretching frequencies[6] and are considered average values.
- We perform geometrical conjugate gradient optimizations (CGOs) of both Co(II) and Co(III) with the spin being fixed to a desired value. This is used to obtain the equilibrium geometries (EQ-GEOs) and the PES. The EQGEOs are optimized or relaxed geometries, where the forces on cobalt and all the amines are below the chosen tolerance $0.01 eV/\text{\AA}$. As for the PESs calculations, we constrain the maximum size of a CG step to be 0.001\AA in order to provide a large sequence of energies. The resulting total energy can subsequently be plotted as a function of the Co-N bond length averaged over the six ligands. In the case of JT dis-

direction, r_{ax} , and the average Co-N bond length in the equatorial plane, r_{eq} , are more reasonable choices.

B. Calculation of potential energy surfaces

In the following we describe the procedure of how we obtained the PES plots in figures 2 and 3.

Figure 2 shows the ground state ($S=0$) and excited state ($S=1$) PESs of Co(III). For the ground state PES we started a CGO at the Co(II, $S=3/2$) EQGEO, denoted as starting point (1), but with the spin fixed to $S=0$ and charge $+3e$. For the excited state PES ($S=1$) we started CGOs at both the EQGEOs of Co(III, $S=0$), starting point (2), and Co(II, $S=3/2$) (not shown for clarity). The vertical arrow indicates the optical excitation energy from the Co(III, $S=0$) EQGEO, where it is assumed that the excited state is initially not JT distorted, since the excitation is almost instantaneous. The dotted line in figure 2 corresponds to total energy versus the average Co-N bond length. Since Co(III, $S=1$) is JT unstable, we also plot the total energy versus the average axial Co-N bond length, r_{ax} , and the average equatorial Co-N bond length, r_{eq} , shown by dashed lines. One can see that essentially only r_{eq} changes when starting a CGO from the Co(III, $S=0$) EQGEO.

In order to obtain smooth PESs it is essential to treat the amines as rigid bodies. If one relaxes all the atoms, the resulting PES would be much more complicated, i.e. the PES would display a sequence of short parabolic curves stemming from periods of contracting or stretching the N-H bond lengths, or from changing the H-N-H angles. The resulting PES would not resemble smooth parabola-like curves (at least for the non-JT distorted ground states) anymore, since the reaction coordinate would not simply be the change of the Co-N bond length. Although equilibrium energies of the constraint complexes might be higher than the all-atom-relaxed ones, this is not a problem, since we are interested in energy differences and finally in the sum of the Co(II) and Co(III) system energies (overall energy shift which does not affect the rate).

Figure 3 shows the ground state $S=3/2$ and excited state $S=1/2$ PESs of Co(II) as a function of the Co-N bond length averaged over all six ligands. Using an analogue procedure, the Co(II, $S=3/2$) PES results from a CGO starting at the Co(III, $S=0$) EQGEO, (1), where we have fixed the spin at $S=3/2$ and the charge at $+2e$. The dotted line shows the Co(II, $S=1/2$) PES, which was obtained from starting at the non-JT distorted Co(III, $S=0$) and Co(II, $S=3/2$) EQGEOs, (2) and (3) respectively. They stay non-JT distorted. The vertical arrow indicates the optical excitation to the non-JT distorted Co(II, $S=1/2$) state. Starting geometry (4) is JT distorted and hence lower in energy than (1). Further relaxation with the CGO method (dashed curve) lowers the energy to the non-JT distorted state (dotted curve).

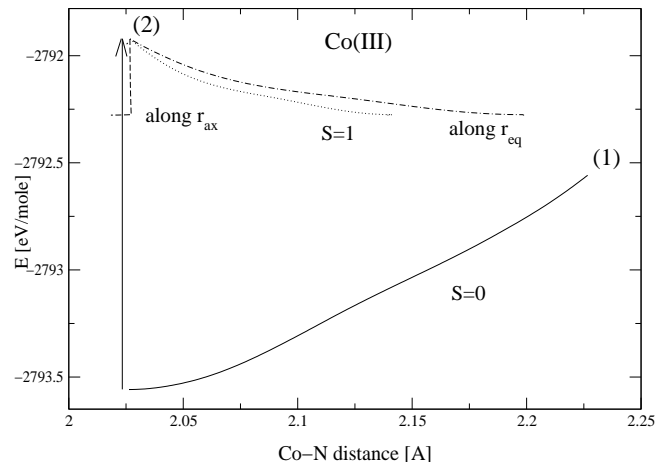


FIG. 2: PESs of Co(III) for spin $S=0$ (solid line) and $S=1$ [\hbar] (dotted line) as a function of the average Co-N bond length. The numbers (1) and (2) indicate the starting points of the CGO. Since Co(III, $S=1$) becomes JT distorted, we also plot the PES along the axial, r_{ax} (dashed line), and equatorial, r_{eq} (dashed-dotted line), average bond length. The vertical arrow indicates the optical excitation discussed in the text.

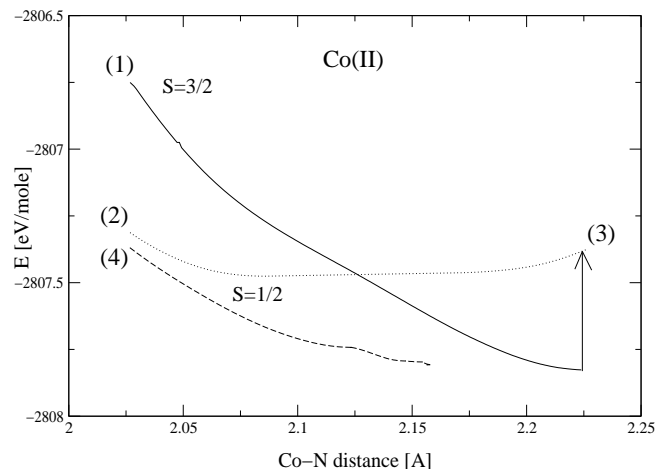


FIG. 3: PESs of Co(II) for spin $S=3/2$ [\hbar] (solid line) and $S=1/2$ (dotted and dashed lines) as a function of the average Co-N bond length. The numbers (1) to (4) indicate the starting points of the CGO. The dotted line shows the non-JT distorted PES, while the dashed line shows a JT distorted PES of Co(II, $S=1/2$). The vertical arrow indicates the optical excitation discussed in the text.

non-JT relaxed energy (dotted curve). The non-JT distorted PES (dotted curve) is hence only meta stable. The energy of the Co(II, $S=1/2$) EQGEO is only 0.3 kcal/mol (less than $k_B T$) higher than the Co(II, $S=3/2$) EQGEO.

Table I contains calculated equilibrium Co-N bond lengths of the ground and excited states and their experimental analogues. For comparison it also shows the ones of the $Co(H_2O)_6^{2+/3+}$ ground states. As typical for the DFT method they are overestimated, about 3% for NH_3 and 2% for H_2O ligands.

TABLE I: Equilibrium Co-ligand bond lengths for cobalt hexaammine and hexaaqua complexes in units of Å. Jahn-Teller (JT) distorted values: r_{ax} denotes the Co-ligand bond length in axial direction, while r_{eq} in the equatorial plane.

	calcd. [Å]	exptl. [Å]
$Co(NH_3)_6^{3+}$	1A_g	2.03
JT distorted $^3T_{1g}$	$r_{ax} = 2.01$ $r_{eq} = 2.20$	1.96[3]
$Co(NH_3)_6^{2+}$	$^4T_{1g}$	2.22
JT distorted 2E_g	2E_g $r_{ax} = 2.42$ $r_{eq} = 2.03$	2.16[32]
$Co(H_2O)_6^{3+}$	1A_g	2.02
$Co(H_2O)_6^{2+}$	$^4T_{1g}$	2.25

^ap.447

^bp.441

Table II compares theoretical and experimental optical excitation energies. The excitation energy $^2E_g \leftarrow ^4T_{1g}$ for $Co(NH_3)_6^{2+}$ is not known from experiment but is very important. If this energy separation is low enough Co(II,S=1/2) is well-populated at ambient temperatures and the electron transfer reaction is spin-allowed. Although absolute excited state energies from DFT cannot be trusted, trends established from DFT are often correct. From table II we can obtain the following. Since DFT underestimates optical gaps such as the D_q ligand-field, DFT favors high-spin compounds. For instance, the ligand-field splitting of Co(III) is 274 kJ/mol[35] while SIESTA gives 246 kJ/mol. In other words, excitations from low-spin to high-spin ($^3T_{1g} \leftarrow ^1A_g$) are underestimated while excitations from high-spin to low-spin ($^2E_g \leftarrow ^4T_{1g}$ and $^4T_{1g} \leftarrow ^6A_{1g}$) are overestimated. Similar results were found for singlet-triplet gaps of phenyl-nitrene and other hypovalent systems[36].

Unfortunately, in the case of low-spin to high-spin excitations there is only one reliable value for Co(III) and no experimental value available for $Co(H_2O)_6^{3+}$ in order to confirm the trend. Nevertheless, we can easily see that the calculated gap for $Co(H_2O)_6^{3+}$ (7,150 cm^{-1}) has to be a lower bound analogous to Co(III). The argument is as follows. From ligand-field theory the excitation energy $^3T_{1g} \leftarrow ^1A_g$ is additive in the ligand field D_q , which is about 25% larger for NH_3 compared to H_2O [22]. Taking a value $D_q = 274kJ/mol$ for Co(III) [35] and 200 kJ/mol for $Co(H_2O)_6^{3+}$ [37], we can correct the excitation energy of Co(III), 13,700 cm^{-1} , by the D_q -difference and obtain an approximate value for $Co(H_2O)_6^{3+}$, 7,500 cm^{-1} . This is clearly higher than the calculated value 7,150 cm^{-1} . Having this trend established we can conclude that the excitation $^2E_g \leftarrow ^4T_{1g}$ of $Co(NH_3)_6^{2+}$, 3,680 cm^{-1} , is an upper bound on the real value.

A further confirmation of the quality of our excitation energy of Co(II) comes from the fact that our value is similar to Larsson's with INDO-CI (3,100–4,100 cm^{-1} after

TABLE II: Spin-forbidden transition energies in units of 10^3cm^{-1} .

$^3T_{1g} \leftarrow ^1A_g$	$Co(H_2O)_6^{3+}$	$Co(NH_3)_6^{3+}$	low-spin to high-spin
calcd.	7.15	13.23	to
exptl.	(> 1.89[15]) ^a	13.70[23] ^b	high-spin
$^2E_g \leftarrow ^4T_{1g}$	$Co(H_2O)_6^{2+}$	$Co(NH_3)_6^{2+}$	high-spin to low-spin
calcd.	8.46	3.68	to
exptl.	≈ 6.4 [33] ^c	–	low-spin
$^4T_{1g} \leftarrow ^6A_{1g}$	$Fe(H_2O)_6^{3+}$		
calcd.	19.01		
exptl.	14.22[34] ^d		

^afrom Cobalt-59 NMR fraction of high-spin < 10⁻⁴. This is not an order of magnitude estimate, but a true upper bound set by experimental resolution.

^bcorresponds to the maximum of the optical absorption peak at $T = 8K$ which stems from a vertical transition in line with the classical Franck-Condon principle.

^cfrom a fit of a four parameter octahedral ligand-field theory (Dq, B, C, λ) including spin-orbit coupling to a circular dichroism spectrum of $[Zn(H_2O)_6]SeO_4$ doped by $Co(H_2O)_6^{2+}$ at $T = 80K$. Ligand-field theory is rather good for electronegative ligands such as oxygen.

^dfrom ions doped into beryl crystal

TABLE III: Energy difference $\Delta E^{3+(2+)}(r)$ in units of 10^3cm^{-1} at the equilibrium position $r_{3+(2+)}^0$ of Co(III,S=0) (Co(II,S=3/2)) and at the transition state r^\dagger of the conventional spin-forbidden process. The values of r^\dagger of this work, Larsson's, and Newton's are 2.09, 2.03, and 2.14 Å, respectively.

		r_{2+}^0	r^\dagger		r_{3+}^0	r^\dagger
this work ^a	ΔE^{3+}	13,23	9.09	ΔE^{2+}	3,68	-1.19
Larsson ^b [22]		13,7	12.0		3,1-4,1	$\lesssim 0$
Newton ^c [8]		13,7	8,8		9,1	5,3

^aDFT-GGA method, the ΔE^{2+} value is w.r.t. non-JT distorted Co(II, S=1/2).

^bINDO-CI method, empirically corrected energies by Eqs. (5,6) with $c = 1, 100cm^{-1}$, energy difference $\Delta E^{3+}(r^\dagger)$ is estimated from their Fig. 5

^cUHF+UMP2 method, empirically corrected energies by Eqs. (5,6) with $c = -6, 000cm^{-1}$

the JT distorted Co(II,S=1/2) equilibrium energy is only slightly higher than the non-JT distorted Co(II,S=3/2) equilibrium energy. Since the S=1/2 PESs are likely too high by a constant energy shift, Co(II,S=1/2) could be close to degenerate with Co(II,S=3/2) or even be the true ground state. Note that these considerations do not include multiplet-splitting due to spin-orbit coupling, as well as entropy effects on the energy ($\sim -TS = -k_B T \ln(g)$, where g is the degeneracy of the multiplet).

In table III we compare the important quantity $\Delta E^{3+/2+}(r)$ from Eqs. (3/4) for various bond lengths r between this, Larsson's[22] and Newton's[8] work. $\Delta E^{3+/2+}(r_{3+/2+}^0)$ are the excitation energies out of the equilibrium states Co(III,S=0)/Co(II,S=3/2) to Co(II,S=1)/Co(II,S=1/2) and $\Delta E^{2+(3+)}(r^\dagger)$ is the

energy difference at the spin-forbidden transition state. The excited state Co(III, S=1) is always much too high in energy to be relevant and is not important for further consideration. However, the value and sign (!) of $\Delta E^{2+}(r^\ddagger)$ decides whether the process will be spin-forbidden (allowed by weak spin-orbit coupling) ($\Delta E^{2+} > 0$), or whether it is spin-allowed ($\Delta E^{2+} < 0$). The former process can be described by second order perturbation theory[6, 8, 12] using Co(II, S=1/2) as a virtually excited state coupled to at the spin-forbidden TS, the latter one is through direct coupling and does not involve spin-orbit coupling[22]. As one can see our value is $\Delta E^{2+}(r^\ddagger) < 0$ and hence the reaction along the lowest energy pathway is spin-allowed.

Figure 4 shows the PES of the total 2 Co-system, i.e. the sum of the single complex energies. The minimum in the left top corner at $(r_L = 2.03\text{\AA}, r_R = 2.22\text{\AA})$ corresponds to equilibrium $\text{Co}_L(\text{III})\text{Co}_R(\text{II})$, where the subscripts L and R stand for “left” and “right”, respectively, and simply distinguish the two complexes. The minimum in the right bottom corner at $(r_L = 2.22\text{\AA}, r_R = 2.03\text{\AA})$ corresponds to equilibrium $\text{Co}_L(\text{II})\text{Co}_R(\text{III})$. The variables r_L and r_R are the Co-N bond lengths of the left and right complex. For simplicity we can only show the non-JT distorted complexes, since a single JT distorted complex depends on two variables, r_{ax} and r_{eq} . This would resolve in a total energy which depends on more than two variables and cannot be plotted. Part A is plotted using the ground state Co(III, S=0) (solid line in Fig. 2) and Co(II, S=1/2) for Co(II)-N bond length $r_2 < 2.125\text{\AA}$ (dotted line in Fig. 3) and Co(II, S=3/2) for $r_2 > 2.125\text{\AA}$ (solid line in Fig. 3). This is an example (by not including JT distorted complexes of lower energy) of a spin-allowed reaction. However, if we restricted ourselves to the O_h group, this would be the lowest energy pathway. Such a reaction starts out at equilibrium $\text{Co}_L(\text{II, S} = 3/2)\text{Co}_R(\text{III, S} = 0)$, then activated by thermal fluctuations changes to the $\text{Co}_L(\text{II, S} = 1/2)\text{Co}_R(\text{III, S} = 0)$ PES at $(r_L = 2.125\text{\AA}, r_R = 2.03\text{\AA})$ through spin-orbit coupling in only first order (presumably adiabatic). Coming back to figure 4, part B shows the PES of Co(III, S=0) and Co(II, S=3/2) and hence describes the conventional spin-forbidden reaction with an energetically higher transition state.

In the following we have to obtain the activation barrier of the reaction. In figure 5 the transition states for spin-allowed (lower graph) and spin-forbidden (upper graph) are plotted. The graphs are the cross-section of the 2Co-PES from figures 4 A and B along the diagonal $r := r_L = r_R$, i.e. $E(r_L = r, r_R = r) = E_{\text{Co(III)}}(r) + E_{\text{Co(II)}}(r)$, where the Co-N bond lengths r_L and r_R are the bond lengths of the “left” and “right” complex. The transition state is defined as the saddle point. Using non-JT distorted Co(II, S=1/2) leads to a lowering of the spin-forbidden transition state by $0.3\text{eV} = 6.92\text{kcal/mol}$. The spin-allowed and spin-forbidden TSs are at $r = 2.05$ and 2.1\AA , respectively. In the next section we use the

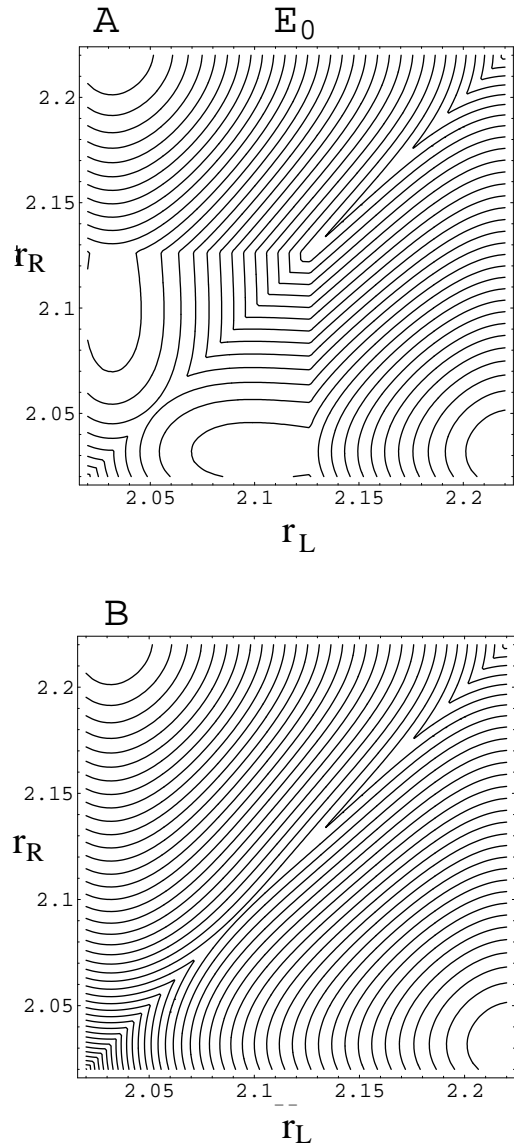


FIG. 4: Contour plot of the PES of total 2 Co-system with contour level spacing $0.03\text{ eV} = 0.69\text{ kcal/mol}$. Only results from the non-JT distorted complexes are shown. A) Example of a spin-allowed reaction using Co(III, S=0) and non-JT distorted Co(II, S=1/2) for Co(II)-N bond lengths $r_2 < 2.125\text{\AA}$ and Co(II, S=3/2) for $r_2 > 2.125\text{\AA}$ (see Fig. 3). Within the O_h group this is the lowest energy reaction pathway. B) PES of conventional spin-forbidden reaction originating from Co(III, S=0) and Co(II, S=3/2) .

mine self-exchange reaction.

Finally a few things are important to keep in mind. Application of the DFT method to transition metal ions is tricky, even more when one is interested in excited states. There are several well-known deficiencies one has to consider. First, it is well known that DFT suffers from issues in describing transition metal ions [23]. This

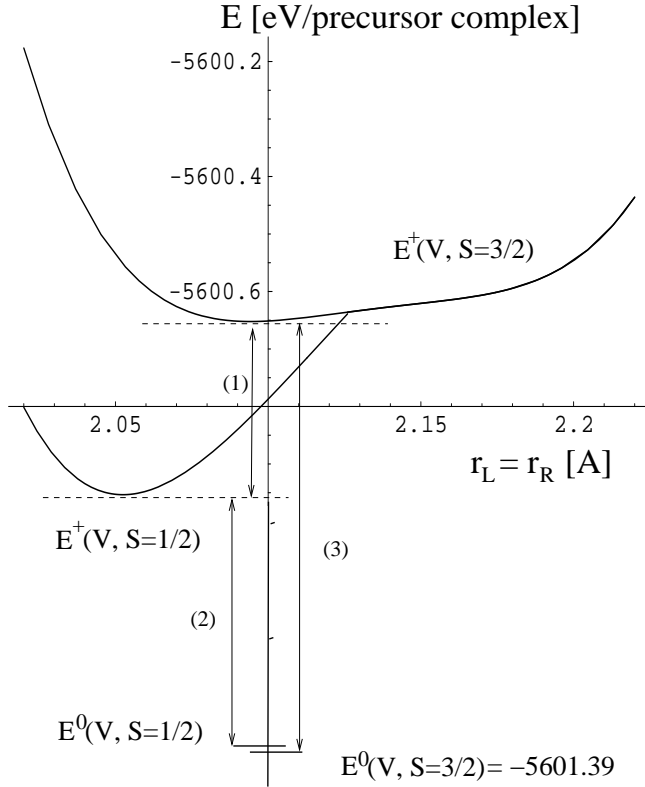


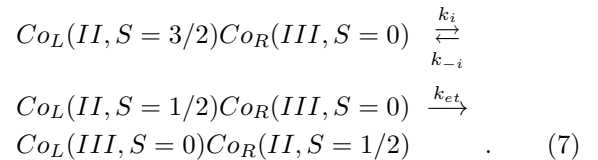
FIG. 5: Cross-section of 2Co-PES, written as $E(\text{total charge in roman letters, total spin})$, along $r_L = r_R$. The TS is defined as the saddle point. Using Co(III, S=0) and non-JT distorted Co(II, S=1/2) lowers the TS by $0.3\text{eV/precursor complex} = 6.92\text{kcal/mol}$ compared to using Co(III) and Co(II, S=3/2) (arrow (1)). Arrows (2) and (3) indicate the two activation barriers being the difference between the energy at the transition state (superscript †) and at the EQGEO (superscript 0).

concerns mainly the localized d-orbitals of cobalt, where the large $d-d$ Coulomb interaction introduces local correlations that are not captured properly by the GGA functional. The second deficiency concerns optical gaps which are generally underestimated[38, 39, 40]. In our case the excited states involve the ligand-field spitting. This, however, is turned to our advantage by using it to deduce a trend. It is utilized in the next section to obtain an essential lower bound on the rate constant. More importantly, since DFT is a ground state theory, we expect that excitation energies obtained from total energy differences (ΔSCF method) are rather reliable. Very good results have been obtained for optical spin (singlet-triplet)[41] and charge[42] excitations. Furthermore, total energies are expected to be better for strongly σ -donating NH_3 than for weakly π -donating H_2O ligands, because the NH_3 ligands are less electro-negative and bind more covalently with cobalt e_g orbitals. Covalent molecular-type systems are well described by the DFT method. Besides, covalency screens the on-site repulsion of the localized

IV. RESULTS

In this section we give an estimate for the hexaamine self-exchange rate using previously estimated electron transfer parameters and results from last section. For now, we take the energies obtained from the DFT calculations literally. For instance, we assume that high-spin Co(II, S=3/2) is the groundstate according to our calculation (see Fig. 3). However, since DFT stabilizes high-spin Co(II, S=3/2) over low-spin Co(II, S=1/2) according to our trend, this rate estimate is a lower bound. This is because we first have to thermally excite to the reaction intermediate, Co(II, S=1/2) , which lowers the rate. With regard to our trend, Co(II, S=1/2) could be the true groundstate.

The initial rate constant to the intermediate state $\text{Co(II, S=1/2)Co(III, S=0)}$ is denoted by k_i . In thermal equilibrium the return reaction with rate constant k_{-i} back to the groundstate $\text{Co(II, S=3/2)Co(III, S=0)}$ is equal to k_i . From the intermediate state the spin-allowed electron transfer can occur with rate constant k_{et}



The resulting total rate constant is k . Since the two steps from Eq. 7 are incoherent due to relaxation along the surfaces, the total rate k can equivalently be described as starting out at the thermally populated (with probability P) intermediate, $\text{Co}_L(\text{II}, S = 1/2)\text{Co}_R(\text{III}, S = 0)$, from where the spin-allowed electron transfer can occur to $\text{Co}_L(\text{III}, S = 0)\text{Co}_R(\text{II}, S = 1/2)$ with rate k_{et} . This does not require rate constant k_i . Hence, the total spin-allowed reaction rate constant is

$$k = P k_{et} = \frac{g e^{-\beta\Delta G^*}}{Z} k_{et} \quad (8)$$

with k_{et} being the electron transfer rate Eq. (2). The prefactor or probability P applies in the case that Co(II, S=1/2) is the excited state, which has first to be thermally populated. $\Delta G^* = \Delta E^* - T\Delta S$ is the free energy of excitation and Z is the partition function.

There are **two main differences** from previous rate estimates:

- Co(II, S=1/2) and Co(II, S=3/2) are nearly degenerate, i.e Co(II, S=1/2) is slightly higher in energy than Co(II, S=3/2) but is probably overestimated. In order to get a lower bound of the rate we hypothetically trust the DFT energies and calculate $\Delta G^* = 0.3\text{kcal/mol} + k_B T \ln(12/4) = 3.1\text{kcal/mol}$ from the energy and the entropy differences between Co(II, S=1/2) and Co(II, S=3/2) . Hence, the prefactor of equation (8) is 0.09 using the degeneracies g from figure 1 and neglecting multiplet-

- The TS of the Co(II,S=1/2)Co(III,S=0) system is *lower* than the TS of Co(II,S=3/2)Co(III,S=0). The inner-sphere contribution to the activation barrier, the energy difference of the 2 Co-system between the TS and equilibrium using Co(II,S=1/2), is only $E_{in}^\dagger = 0.42eV = 9.69kcal/mol$. For the equilibrium energy of Co(II,S=1/2), we take the JT distorted value, for TS we use the non-JT distorted one. This seems reasonable, because the acceptor, Co(III,S=0), is non-JT distorted. In order to have sufficient nuclear overlap, the donor should be non-JT distorted at TS, too.

The other parameters are only slightly modified. This is mainly due to using a different nuclear frequency for Co(II), i.e. $\nu_2(E_g)$ for Co(II,S=1/2) instead of $\nu_2(A_{1g})$ for Co(II,S=3/2):

The **product** $K_{equ}\nu_{eff} = 1.4 - 3 \cdot 10^{11}(Ms)^{-1}$ has been estimated before for the spin-forbidden process by Sutin [6] and Newton[8, 12] using a preequilibrium constant $K_{equ} = 0.013M^{-1}$ and an effective nuclear frequency $\nu_{eff} = 347cm^{-1}$ [8]. Since the case at hand is slightly different (low-spin Co(II,S=1/2)), we redetermine ν_{eff} . The average harmonic frequency is given by[6, 43, 44]

$$\nu_{eff}^2 = \frac{\nu_{solv}^2 E_{solv}^\dagger + \nu_{in}^2 E_{in}^\dagger}{E_{solv}^\dagger + E_{in}^\dagger}, \quad (9)$$

where $\nu_{in} = \sqrt{2\nu_2\nu_3}/\sqrt{\nu_2^2 + \nu_3^2}$ is the reduced inner-sphere nuclear frequency of Co(II) and Co(III). Using the experimental values $\nu_2(E_g) = 255cm^{-1}$ and $\nu_3(A_{1g}) = 494cm^{-1}$ [11], respectively we obtain $\nu_{in} = 320cm^{-1} = 9.6 \cdot 10^{12}s^{-1}$. For the solvent, we use a typical value $30cm^{-1} = 0.9 \cdot 10^{12}s^{-1}$ [44]. We do not attempt to estimate $\nu_{2/3}$ from the PESs due to complications from JT distortions in the case of Co(II,S=1/2). The outer-sphere, $E_{out}^\dagger = 28/4kcal/mol = 7kcal/mol$, was previously determined by Buhks and colleges applying the Marcus-Levich continuum model for the solvent[11, 12]. We neglect entropy contributions, which are quite small for water near room temperature[43] and vanish for the inner-sphere system, if the (harmonic) vibrations are the same for the activated complex and the reactants[6]. Using these parameters, one obtains $\nu_{eff} = 245cm^{-1} = 7.3 \cdot 10^{12}s^{-1}$ and $K_{equ}\nu_{eff} = 9.5 \cdot 10^{10}(Ms)^{-1}$.

The **electronic transmission coefficient** for the e_g -transfer was determined by Larsson and colleges to be weakly adiabatic, $\kappa_{el} \approx 0.5$ [22], using parameters for the spin-forbidden process and standard Landau-Zener theory[45]. Extended Hückel theory was applied to calculate the donor(D)-acceptor(A) electronic coupling, $H_{DA} = {}_D\langle e_g | H | e_g \rangle_A$, for different precursor complexes (apex-to-apex, apex-to-edge, apex-to-side). A subsequent orientational averaging gave $\bar{H}_{DA} \approx 200cm^{-1}$. Their statistical analyses assumes that each complex can rotate independently and that each configuration covers the same probability. The Co(II,S=1/2) complex has a

7\AA (van der Waals contact between first solvation shells), the Co-N distances of both complexes were fixed at 2.06\AA reasonably close to our TS value, 2.05\AA . A similar procedure was applied by Newton[8]. Utilizing \bar{H}_{DA} from above, our parameters E_{solv}^\dagger , E_{in}^\dagger , $\nu_{in/eff}$ and Eqs. (7-11) from Ref.[8, 46], we redetermine the electronic transmission and nuclear tunneling factors and obtain adiabaticity $\kappa_{el} = 0.73$ and weak nuclear tunneling $\Gamma_n = 1.9$, respectively.

Finally, the **activation barrier** has inner-sphere and outer-sphere contributions and is lowered by the average electronic coupling at TS, i.e. $G^\dagger \approx E^\dagger = E_{in}^\dagger + E_{solv}^\dagger - \bar{H}_{DA}$, and is given by $G^\dagger = 0.70eV = 16.0kcal/mol$. This leads to a Boltzmann factor $e^{-\beta G^\dagger} = 2.1 \cdot 10^{-12}$. Including all the calculated charge transfer parameters in Eq. (8) gives a rate constant of $6 \cdot 10^{-3}(Ms)^{-1}$, which is about 2 orders of magnitude larger than experiment. Possible sources of errors are discussed in section V.

In the following, we again want to stress the main differences between our treatment of a spin-allowed process and the conventional spin-forbidden reaction by Buhks *et al.* and Newton[8]. The main difference is that in our case the low-spin Co(II,S=1/2) complex has a lower energy than the high-spin Co(II,S=3/2) near the TS as opposed to Buhks *et al.* and Newton. In their case, the spin excited state Co(II,S=1/2) is much higher in energy and is only virtually coupled to by weak spin-orbit coupling. This leads to extremely small rates of order $10^{-10}(Ms)^{-1}$. In table IV we show for further illustration the individual parameters used to calculate the rate according to Eqs. (2) and (8) and compare to Newton's spin-forbidden and hence diabatic groundstate reaction and thermally excited adiabatic pathway. The spin-forbidden reaction is significantly lowered by the weak spin-orbit coupling ($\kappa_{el} \ll 1$), while the excited alternative is thermally not accessible and leads to even smaller rates. The ${}^2E_g \leftarrow {}^4T_{1g}$ excitation energy is as large as $9,100cm^{-1}$, while in our case it is only $3,680cm^{-1}$.

V. DISCUSSION

At this point, there are two main possibilities why there is a 2 order of magnitude disagreement between our, $6 \cdot 10^{-3}(Ms)^{-1}$, and the experimental rate, $5 \cdot 10^{-5}(Ms)^{-1}$. Either something is not correct with the theoretical estimate, or the experimental rate constant is too small. In the more likely case that the theory misses some details, the sources of possible errors are the ${}^2E_g \leftarrow {}^4T_{1g}$ excitation energy and hence the prefactor of Eq. (8). Increasing the energy of the Co(II,S=1/2) PESs w.r.t. Co(II,S=3/2) by a constant energy shift $2,560cm^{-1}$ and hence increasing the excitation energy to $6,240cm^{-1}$, produces the experimental value. This, however, is in conflict with the trend of excitation energies established from the DFT method.

TABLE IV: Rate parameters (see Eqs. (2) and (8)) used in this (spin-allowed) and Newton’s (spin-forbidden and thermally excited) work. The rates are compared with experimental estimates. (!) indicates main differences between Newton’s and our work.

	g/Z	K_{equ}	$\nu_{eff}[cm^{-1}]$	κ_{el}	Γ_n	$\Delta G^\ddagger[kcal/mol]$	rate $k[(Ms)^{-1}]$
exp.[3, 4, 10]							$10^{-7} - 10^{-5}$
this work	0.28	0.013	245	0.73	1.9	16.3 ^a	$6 \cdot 10^{-3}$
Newton ^b [8]:							
thermally excited		0.013	245	0.67	2.4	30.7(!) ^c	$2 \cdot 10^{-11}$
spin-forbidden		0.013	347	10^{-4} (!) ^d	9	24.4	$4 \cdot 10^{-10}$

^aincludes ΔG^* from Eq. (8)

^bindividual parameters are presented to the best of our knowledge

^cdue to a large ${}^2E_g \leftarrow {}^4T_{1g}$ excitation energy of $9,100cm^{-1}$

^ddue to a spin-orbit reduction factor of $\gamma^2 = 1.8 \cdot 10^{-4}$.

originate from a more complicated cross-over from the JT distorted Co(II,S=1/2) equilibrium complex to thermally excited non-JT distorted Co(II,S=1/2) near TS. The cross-over could be rather unlikely, since the symmetry changes.

On the other hand, possible experimental issues are beyond our realm of knowledge. Although a difficult experiment, it has been thoroughly studied over decades. Nevertheless, generally forgotten, neglected or underestimated side-reactions lead to an underestimation of the rate constant. In particular, the existence of high-spin Co(II,S=3/2) is challenged by our analysis. This leads to the question, if the assumption of high-spin Co(II,S=3/2) was wrongly made when deriving certain rates of side-reactions. Having said this, an error of about 2 orders of magnitude in the rate estimate is not as bad as it may sound. Due to the activated nature of the reaction, the exponential dependence of the rate on the activation barrier and excitation energy makes it very sensitive to small errors.

VI. CONCLUSION

Within Marcus theory of charge transfer the rate constant of the hexaamminecobalt-self-exchange reaction was redetermined. We utilized the DFT code SIESTA to calculate Born-Oppenheimer potential energy surfaces and spin-excitation energies and use previously determined parameters. The main differences from former work is the near degeneracy of Co(II,S=3/2) and Co(II,S=1/2). Furthermore, we observed a drastic lowering of the activation barrier ($\sim 6.9kcal/mol$)

for the reaction pathway involving and Co(III,S=0) and Co(II,S=1/2). This led to a rate constant of order $6 \cdot 10^{-3}(Ms)^{-1}$ which is 2 orders of magnitude faster than experiment. Possible sources of errors are outlined in section V and having most likely to do with the neglect of the proper cross-over treatment from Jahn-Teller distorted equilibrium Co(II,S=1/2) to non-Jahn-Teller distorted Co(II,S=1/2) near the transition state. The good quality of our energetics involved in the rate constant evaluation is indicated, first because our calculated excitation energy $13,230cm^{-1}$ of Co(III), ${}^3T_{1g} \leftarrow {}^1A_g$, agrees well with the experimental value $13,700cm^{-1}$. Second, our excitation energy $3,680cm^{-1}$ of Co(II), ${}^2E_g \leftarrow {}^4T_{1g}$, is close to Larsson’s value from INDO-CI ($3,100 - 4,100cm^{-1}$). This energy is in particular important for charge transfer. Unfortunately, the corresponding optical absorption peak could not be found experimentally. This may simply be explained by the spin-forbiddensness and vibrational broadening because of differences in equilibrium Co-N bond distances and a Jahn-Teller unstable excited state. On the other hand, our analysis questions the existence of the high-spin ground state Co(II,S=3/2) and hence can provide an alternative explanation for the absence the the absorption peak.

Acknowledgement. We would like to thank P. Ordejón, E. Artacho, D. Sánchez-Portal and J. M. Soler for providing us with their *ab initio* code SIESTA. This work at Davis was supported by the U.S. Department of Energy, Office of Basic Energy Sciences, Division of Materials Research, and also received support from NSF IGERT “Nanomaterials in the Environment, Agriculture, and Technology”.

[1] D. R. Stranks, Diss. Faraday Soc. **29**, 73 (1960); N. S. Biradar, D. R. Stanks, M. S. Vaidya, Trans. Faraday Soc. **58**, 2421 (1962)

[2] R. A. Marcus, J. Phys. Chem. **67**, 853 (1963)

[3] D. Geselowitz and H. Taube, Adv. Inorg. Bioinorg. Mech. **1**, 391 (1982)

[4] A. Hammershoi, D. Geselowitz, and H. Taube, Inorg. Chem. **23**, 979 (1984)

[5] B. S. Brunschwig *et al*, Faraday Discuss. Chem. Soc. **74**, 113 (1982)

[6] N. Sutin, Prog. Inorg. Chem. **30**, 441 (1983)

[7] R. A. Marcus and N. Sutin, Biochim. Biophys. Acta. **811**,

- 265 (1985)
- [8] M. D. Newton, *J. Phys. Chem.* **95**, 30 (1991)
- [9] W. B. Lewis, C. D. Coryell, and J. W. Irvine, Jr., *J. Chem. Soc.*, S386 (1949); F. P. Dwyer and A. M. Sargerson, *J. Phys. Chem.* **65**, 1892 (1961)
- [10] J. J. Grossman and C. S. Garner, *J. Chem. Phys.* **28**, 268 (1958)
- [11] E. Buhks, M. Bixon, J. Jortner, and G. Navon, *Inorg. Chem.* **18**, 2014 (1979)
- [12] M. D. Newton, *J. Phys. Chem.* **90**, 3734 (1986)
- [13] W. Kohn, A. D. Becke, and R. G. Parr, *J. Phys. Chem.* **100**, 12974 (1996); and references therein
- [14] D. Sánchez-Portal, P. Ordejón, E. Artacho, and J. M. Soler, *Int. J. Quantum Chem.* **65**, 453 (1997); E. Artacho, D. Sánchez-Portal, P. Ordejón, A. Garcia, and J. M. Soler, *Phys. Status Solidi (b)* **215**, 809 (1999); P. Ordejón, E. Artacho, and J. M. Soler, *Phys. Rev. B* **53**, R10441 (1996)
- [15] G. Navon, *J. Phys. Chem.* **85**, 3547 (1981)
- [16] N. E. Kime and J. A. Ibers, *Acta Cryst. B* **25**, 168 (1969)
- [17] D. T. Richens, *The chemistry of aqua ions*, (John Wiley and Sons, Chichester and New York, 1997), pp.442,450
- [18] R. A. Marcus, *J. Chem. Phys.* **24**, 966 and 979 (1956); B. S. Brunschwig, J. Logan, M. D. Newton, and N. Sutin, *J. Am. Chem. Soc.* **102**, 5798 (1980)
- [19] W. F. Libby, *J. Phys. Chem.* **56**, 863 (1952)
- [20] L. E. Orgel, *Rep. Solvay Conf. Chem.*, 10th, 329 (1956)
- [21] H. C. Stynes and J. A. Ibers, *Inorg. Chem.* **10**, 2304 (1971)
- [22] S. Larsson, K. Stahl, and M. C. Zerner, *Inorg. Chem.* **25**, 3033 (1986)
- [23] R. B. Wilson and E. I. Solomon, *J. Am. Chem. Soc.* **102**, 4085 (1980)
- [24] W. P. Anderson, W. D. Edwards, and M. C. Zerner, *Inorg. Chem.* **25**, 2728 (1986)
- [25] N. Troullier and J. L. Martins, *Phys. Rev. B* **43**, 1993 (1991)
- [26] L. Kleinman and D. M. Bylander, *Phys. Rev. Lett.* **48**, 1425 (1982)
- [27] S. G. Louie, S. Froyen, and M. L. Cohen, *Phys. Rev. B* **26**, 1738 (1982)
- [28] O. F. Sankey and D. J. Niklewski, *Phys. Rev. B* **40**, 3979 (1989)
- [29] J. P. Perdew, K. Burke, and M. Ernzerhof, *Phys. Rev. Lett.* **77**, 3865 (1996)
- [30] O. Gunnarsson and B. I. Lundqvist, *Phys. Rev. B* **13**, 4274 (1976)
- [31] R. O. Jones and O. Gunnarsson, *Rev. Mod. Phys.* **61**, 689 (1989)
- [32] A. W. Herlinger, J. N. Brown, M. A. Dwyer, and S. F. Pavkovic, *Inorg. Chem.* **20**, 2366 (1981)
- [33] K. D. Gailey and R. A. Palmer, *Chem. Phys. Lett.* **13**, 176 (1972)
- [34] G. G. Hammes and M. L. Morell, *J. Am. Chem. Soc.* **86**, 1497 (1964)
- [35] D. A. McQuarrie and P. A. Rock, *General Chemistry, Third Edition*, (W. H. Freeman and Company, New York, 1991), p.1013
- [36] B. A. Smith and C. J. Cramer, *J. Am. Chem. Soc.* **118**, 5490 (1996); and references therein
- [37] D. A. Johnson and P. G. Nelson, *Inorg. Chem.* **38**, 4949 (1999)
- [38] P. Fulde, *Electron Correlations in Molecules and Solids, Third Edition*, (Springer, Berlin, Heidelberg, New York, 1995), p.51
- [39] V. I. Anisimov, F. Aryasetiawan, and A. I. Lichtenstein, *J. Phys. Condens. Matter* **9**, 767 (1997)
- [40] S. G. Louie, in *Topics in computational material science*, ed. C. Y. Fong (World Scientific, Singapore, London, 1998), Chap. 3
- [41] C. J. Cramer and F. J. Dulles, *J. Am. Chem. Soc.* **116**, 9787 (1994)
- [42] C. Massobrio, A. Pasquarello, and R. Car, *Phys. Rev. Lett.* **75**, 2104 (1995)
- [43] M. D. Newton, *Int. J. Quan. Chem. Symp.* **14**, 363 (1980)
- [44] B. S. Brunschwig, C. Creutz, D. H. Macartney, T-K. Sham, and N. Sutin, *Faraday Diss. Chem. Soc.* **74**, 113 (1982)
- [45] L. D. Landau, *Phys. Z. Sowjetunion* **1**, 88 (1932); **2** 46 (1933); C. Zener, *Proc. R. Soc. London A* **137**, 696 (1932); **140** 660 (1933)
- [46] Eq. 10 of Ref. [8] misses a factor $(h\nu_{eff})^{-1}$.